Internal wave observations off Isle Verte

by R. Grant Ingram[1]

ABSTRACT

A comparison is made between series of high frequency internal waves observed in the St. Lawrence estuary from an aircraft and in a field program at a later date. Wave generation is associated with the propagation of a warm surface front during each ebb flow. The number of waves, as evidenced by surface slicks, is thought to vary as does the stability of the upper layer of the water column.

1. Introduction

On 26 June 1973, an extensive aerial survey of the area near the confluence zone of the St. Lawrence and Saguenay Rivers was conducted. During one of the over-flights a banded pattern was observed in the central region of the South Channel (Fig. 1). Because of the characteristic length separating the individual filaments and other factors, the pattern was thought to result from the presence of internal waves.

Two years later, field observations were taken in the same area over a semi-diurnal tide cycle (Fig. 2). On this occasion only two flotsam lines passed the research ship, progressing in the same direction as the prevailing current. However, the first of these marked the initiation of a series of similarly directed large amplitude internal waves. These waves were observed at a similar tidal phase to that occurring at the time of the aerial observations in 1973.

In this paper the characteristics of the pattern observed in the aerial photographs will be described and related to typical properties of the water masses in the South Channel. Results from the field program are analyzed and the internal wave series described. The relationship between stability of the water column and internal wave presence or absence is discussed.

2. Methods

The aerial observations were made by the Canada Centre for Remote Sensing in June of 1973, using an aircraft flying at about 3050 m above sea level. No ground truth was available in the South Channel during the overflights. Field observations

1. Marine Sciences Centre, McGill University, 3600 University St., Montreal, Que. H3A 2T8, Canada.

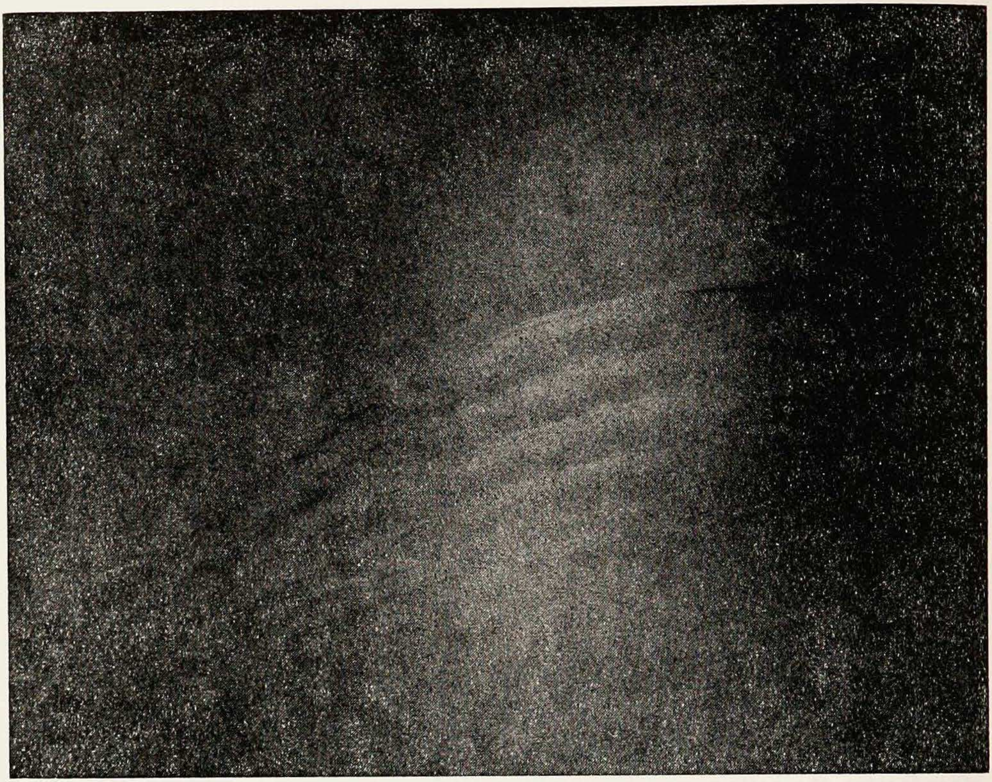

Figure 1. Aerial photograph of banded surface pattern in the South Channel of the St. Lawrence Estuary. Area shown is 4.5 × 3.5 km.

in this area were taken by the Bedford Institute of Oceanography one week after the aerial surveillance.

In June 1975, field studies were carried out on board the M.V. *Metridia.* After anchoring the ship, two Aanderaa current meters (RCM) were positioned at depths of 4 and 9.4 m, with respect to the surface. Profiles of current, temperature and salinity over the water column were done routinely. In addition to the positioning of two current meters at fixed depths, a CTD was placed at a depth of 0.8 m. All instruments were located approximately 3 m off the starboard side of the ship. Sampling time was 30 seconds for the RCM and 5 seconds for the CTD time series. Response time for the RCM thermistor was 1 second, while the CTD platinum resistance thermometer had a time constant of 60 ms. The local water depth at this station was 70 m.

All quoted directions are with respect to magnetic north. Velocity values have been resolved into downstream (55° mag) and cross-channel (325° mag) components.

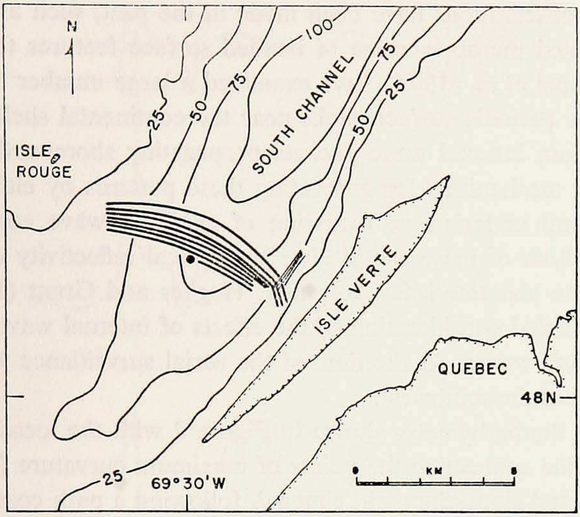

Figure 2. Place map and bathymetry of study area. Location of the observed surface features is shown by the thicker lines off Isle Verte. The large dot corresponds to the position of the 1975 anchor station.

3. Results

Aerial survey. The aerial photograph shown in Figure 1 was taken over the South Channel of the St. Lawrence River, at 1336 EST, 26 June 1973, which corresponded to 3½ hours after high tide. In the center of the picture a distinctive pattern can be seen in mid-channel. The leading point of the first band was located at approximately 48° 03.1′N, 69° 29.7′W. By combining this picture with two others, taken within the following two minutes, a more complete description of the surface phenomena could be obtained, as shown in Figure 2. At this phase of the tidal cycle, the flow is usually downstream, with a magnitude between 30 and 60 cm/sec (Canadian Hydrographic Service, 1939). Assuming this current direction, the mid-channel flow is at right angles with respect to the band orientation.

The individual filaments of the pattern were not evenly spaced, but exhibited a decreasing separation in the upstream direction and a change of curvature. On examining a section of the pattern 2 km offshore of Isle Verte, the distance between sequential bands in the upstream direction was 285, 240, 160 and 150 meters. These features were thought to result from the presence of internal waves propagating in the same direction as the prevailing current. Visualization of the waves may have resulted from convergent surface flow, which would provide flotsam accumulation. An additional feature of the waters in this channel which may provide visual contrast is the large vertical gradient of turbidity (decreasing with depth). This would generate surface turbidity variations in the presence of large internal waves.

Similar aerial observations have been made in the past, such as those by Shand (1953), who related the appearance of banded surface features to internal waves. More recently, Apel *et al.* (1975) have examined a large number of satellite observations that show periodic surface slicks near the continental shelf and interpreted these to result from internal wave packets propagating shoreward. They also discussed two other mechanisms for generating these patterns by either accumulation of surface oils and materials or focussing of capillary wave energy in the convergence zones. Both of these would alter the optical reflectivity of the surface or its light absorption characteristics. Recently, Hughes and Grant (1978) have completed a more detailed consideration of the effects of internal waves on the properties of surface wind waves. At the time of the aerial surveillance wind speeds were 4 to 5 m/sec, out of the southwest.

By comparing the bathymetry shown in Figure 2 with the location and shape of the pattern, the line connecting the points of maximum curvature (critical points) is found to be directed along the main channel, following a path corresponding to the locus of the deepest part of the cross-section. Bands are either not found or are radically changed in character in waters shallower than about 50 m. Adjacent to Isle Verte, a series of closely spaced (< 80 m wavelength) bands can be seen between the 50 m isobath and the shore. The orientation of this pattern is at right angles to that found in the main channel.

Although only one photograph is shown herein, subsequent exposures, overlapping each other by 60%, allowed for a rough calculation of the speed with which the band moved. Assuming a constant aircraft speed over the time interval between photographs, the leading band was propagating at a speed of $\sim$ 80 cm/s. Because of the difficulty in resolving the displacement of the other lines, no estimate of their motion was possible.

Unfortunately, no field observations were taken in the South Channel during the overflight. It was not until 2 July 1973 that CTD observations were taken in this area by the Bedford Institute of Oceanography. As these data were the best available, their general characteristics will be described. At a similar tidal phase as the aerial observations, σ_T values ranged from 21.3 to 25.3 between 0 and 70 m. Although the pycnocline was broad, it could be placed in the 20-25 m depth interval, where the Brunt-Väisälä frequency was $\sim 3.4 \times 10^{-2}$ sec^{-1}. Using these values and a local depth of 70 m, the phase speed of lowest internal mode is $\sim$ 70 cm/sec, assuming a wavelength of 285 m. The wave refraction seen in Figure 1 is consonant with the concept of decreasing phase speeds in shallower areas. The pattern did not extend into depths which are less than about twice the local thermocline depth. Wavelength was large compared to the local thermocline depth for all waves. It might be expected from the work by Lafond (1966) and others that the waves were long crested in depths greater than 50 m and short crested in shallower regions. Alterations to the thermocline might be expected in the near shore areas. In sum-

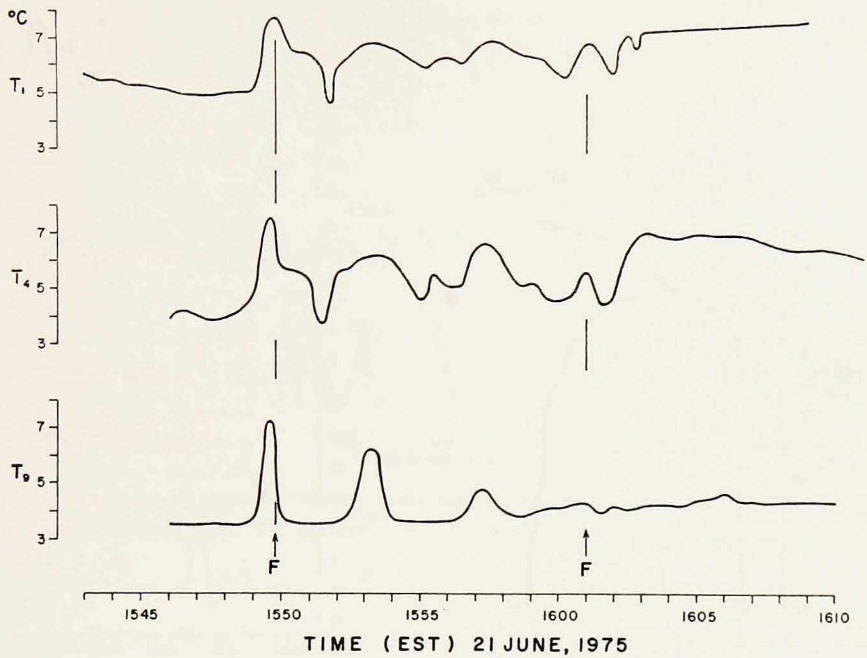

Figure 3. Time series of temperature at 0.8 (T_1), 4.0 (T_4) and 9.4 (T_9) m. *F* corresponds to the arrival of a foam line at the surface.

mary, it is difficult to draw anything more than a tentative relationship between the bands appearing in the photograph and CTD data taken a week later. The shipboard observations were taken on an hourly basis. No mention of a banded pattern passing their vessel was reported.

Field Survey: 21 June 1975. Approximately 3½ hours after high tide, a very long line of flotsam passed our anchored vessel. Its speed of propagation was about 75 cm/s, as determined by the time required for the flotsam to travel the length of the ship. This surface feature advanced at a slight angle (about −20°) with respect to the prevailing current direction. For the visual observations, surface current direction was assumed to be similar to the ship orientation. Winds were negligible at the time of the observations. Thus, the line of flotsam propagated in a downstream direction, as did the local tidal current, but with a larger positive cross-channel component. Thirteen minutes later a less well-defined line of debris passed our ship, propagating at a speed of 95 cm/s.

Temperature observations at depths of 1, 4 and 9.4 m made immediately before and subsequent to the passage of the first flotsam line showed the presence of rapid changes in water mass characteristics in the near surface layer (Fig. 3). Temperatures rose almost 4°C at the lowest level. The foam line appeared to arrive just

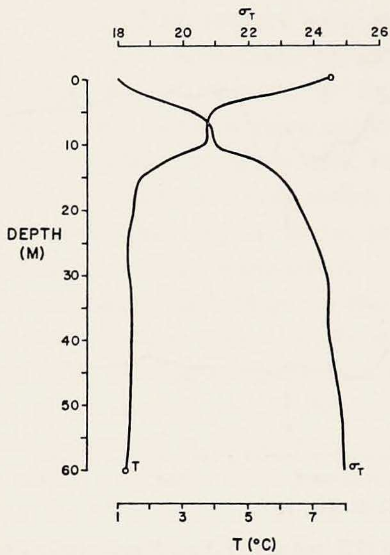

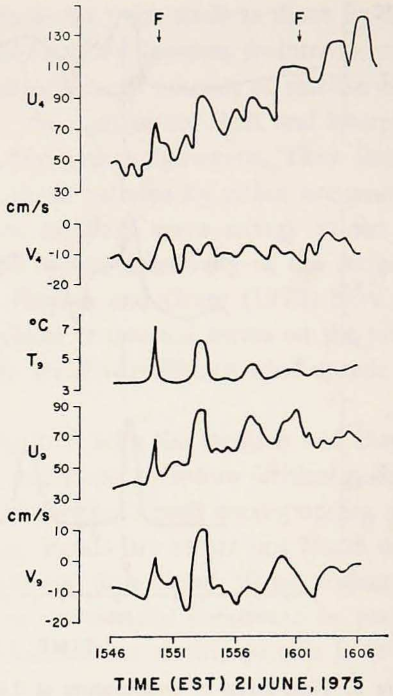

Figure 4. Temperature and sigma-*t* vs depth for anchor station at 1532 EST 21 June 1975.

Figure 5. Time series of down channel (*U*) and cross channel (*V*) velocity with temperature at RCM positions. Similar key as Figure 3.

after the maximum values. However, within our sampling interval, there was no phase lag in depth. Although only one other foam line was seen at the surface, an additional two peaks in the temperature field were observed. As temperature decreased with depth at this site, the first wave could be characterized by a sharp narrow trough and a long flat crest. Subsequent observations showed a transition to short crests and long troughs at 1 and 4 m and no change at the 9.4 m level. Extremes of temperature at the three levels were well correlated, in spite of the change in shape. The signal at 9.4 had the smallest amount of high frequency variability. Although the mean temperature increased at all depths after wave passage, the largest changes were recorded at the upper two levels. The event described above was short-lived, lasting about 14 minutes. The time between peaks at the 9.4 m depth was approximately 4 minutes.

Figure 4 shows the vertical profile for temperature and density taken thirteen minutes before arrival of the first foam line. At this time the water column was well stratified in the upper 25 m. Using these values, peak to peak amplitude of the individual waves pictured in Figure 3 were estimated to be approximately 15, 10 and 4 m (at 9.4 m depth). The Brunt-Väisälä frequency of the upper 10 m was $\sim 5 \times$

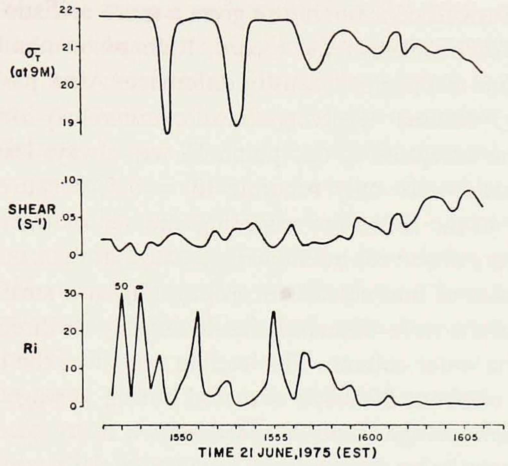

Figure 6. Time series of sigma-*t*, velocity shear and Richardson number. The latter two variables were calculated from the gradients between 4 and 9.4 m. Off scale values are enumerated.

10^{-2} sec^{-1}. Below 20 m, values were less than 3×10^{-2} sec^{-1} (or the equivalent of a period of $\sim$ 4 minutes). A step-like irregularity in the profile can be seen in the 5-10 m depth interval.

Associated with the rapid rise of temperature in the trough was an increase of current speed and a slight change in direction. In Figure 5, the two velocity components for 4 and 9.4 m have been plotted. Although the downstream component (U) increased with time at both levels, one could easily distinguish the peaks in magnitude above the trend. Variations of temperature and U were well correlated. At 9.4 m, bursts of more positive cross-channel velocity (V) occurred at the same time as the peaks in U. A similar response was found only during the passage of the first wave at 4 m. The observed change of current direction (about $-15°$) was consonant with the surface observations. The velocity increment associated with the temperature increase, or wave trough, was of the order 25-30 cm/s at both depths. Although the wave amplitude decreased with time, no similar changes were seen in the velocity variation.

In Figure 5, U was found to increase $\left(\frac{\partial U}{\partial t} \sim .05 \text{ cms}^{-2}\right)$ more rapidly at 4 m than at the lower level. During this same period the salinity values decreased as temperature increased. Thus, both the vertical stratification and shear increased over the observation period. In Figure 6, time series of velocity shear and gradient Richardson number ($\text{Ri} = N^2/(\vec{U}'(z))^2$) are plotted on the same graph as the σ_T values recorded at 9.4 m. N is the Brunt-Väisälä and $\vec{U}'(z)$ is the unsmoothed total velocity shear between 4 and 9.4 m, calculated using both components. Graphing density fluctuations instead of temperature gives a more realistic picture of the wave form in *Z-t* space. At the start of the record, Richardson numbers were lowest in the troughs, as a result of the small density difference. After passage of three waves the shear increased ($> .03$ sec^{-1}), giving almost continuously low values of Richardson number. With the exception of one point, Ri was always less than 1.3 and typically 0.6-0.7. Ri values were only accurate to $\pm$ 0.5, because of the digitization technique employed in the RCM for recording and sensor tolerances. Only two Ri values below 0.35 were observed, both during passage of the troughs.

In summary, a series of internal waves propagating at a small angle with respect to the prevailing current were observed simultaneously at three different depths in the upper 10 m of the water column. The leading wave was the largest in amplitude. A velocity increase of about 30 cm/s occurred during passage of each trough. As the RCM provides an average value of speed over a thirty second interval, the incremental velocity may be underestimated because of the sharp troughed nature of the wave. Waves were not found for conditions of high velocity shear. After wave passage a density decrease was noted in the upper 5 m.

4. Discussion

The large amplitude internal waves observed described above are quite similar to the internal undular surges occurring in Seneca Lake, as described by Hunkins and Fliegel (1973). They found a small number of coherent pulses with broad peaks and sharp troughs which preceded a rapid isotherm deepening. A series of uncorrelated lower amplitude waves followed the deepening. Hunkins and Fliegel interpreted the initial pulses as being solitons of nonlinear wave theory. A similar finding by Lee and Beardsley (1974) was used to explain the large amplitude internal waves, seen by Halpern (1971), behind Stellwagen Bank once every semi-diurnal tide cycle. Gargett (1976) has also examined the generation of high frequency internal waves by abrupt changes of the tidal currents in the Strait of Georgia. The generation mechanism proposed by Lee and Beardsley seems most relevant to the present observations. Initially, a warm front is formed due to partial blocking of a stratified flow over a submarine sill. As the internal front steepens, waves are formed due to the action of dispersion and nonlinearity. These waves evolve into a series of permanent internal solitary waves. As the wave propagation speed is dependent on its amplitude the larger waves are observed first and there is an uneven spacing between individual waves, similar to that recorded in the aerial photos shown earlier. Using Lee and Beardsley's theoretical treatment the characteristic wavelength of the solitons in the St. Lawrence at generation is about 50 m. Since the horizontal separation between the generation and observation site is unknown, prediction of the expected wavelength cannot be made.

Halpern (1971) had observed series of parallel surface bands propagating in the same direction as the tidal current and oriented in the same manner as Stellwagen Bank. In the present case there is no sill directly upstream of South Channel, only a gradual shoaling to a narrow channel. The major ebb flow in this area occurs over an upstream sill, which parallels the downstream estuarine axis, separating the North and South Channel. Thus, the flow is initially directed in a negative cross-channel and positive downchannel direction across a sill, which is at right angles to the general orientation of the surface bands in Figure 1 and that observed in the field. Because of the inappropriateness of these conditions, the generation of the internal front probably occurs from the introduction of less dense water from the shallow region upstream of the South channel upon the heavier waters existing at the end of the previous flood.

On comparing the aerial photos and the field observations, the differing number of surface bands is the most obvious difference. Because of differing wind conditions on the two dates, the effect on surface waves, as discussed by Hughes and Grant (1978), may cause a misinterpretation of the visually observed properties. However, in this instance, there were at least four more waves in the 1973 photo than were actually observed (Fig. 3) in the 1975 field study. Since the local stratification should be similar from year to year, the most evident contrast between existing conditions was the differing phase of the fortnightly tide. The aerial photo was taken during neap tide, while the field work was done at quadrature. This would allow for a contrast in both vertical stratification and mean velocity shear, as baroclinic tidal streams and mixing characteristics would differ. As inferred from Figure 6, the influence of increased shear is to limit the number of waves observed. Tidal range usually varies by a factor of three over the half-fortnightly period. Mean tidal range is 3 m. Thus, it can be seen that conditions suitable for the generation of internal waves are found during each semi-diurnal tide cycle in the South Channel. Furthermore, wave dissipation increases with tidal energy, so that a larger number of waves is found at neap tide. This is thought to result from the less stable conditions existing during higher amplitude tides.

Another noticeable feature in Figure 1 was the wavefront refraction in shallower areas and wave absorption in waters of depths less than 50 m. In the latter locations, the nonlinear expansion parameter, ϵ, of Lee and Beardsley's (1974) analysis becomes greater than 0.5, and cannot be considered small. Excepting these regions, the theory should be applicable as the mean Richardson numbers were all greater than 0.25 between the two layers, corresponding to stable conditions. Even so, no significant internal waves were observed in the field program during conditions of high shear ($> 0.03\ \mathrm{sec}^{-1}$).

In summary, a series of long internal waves is generated in the South Channel of the St. Lawrence estuary during the ebb flow, 3½ hours after high tide. The theoretical argument proposed by Lee and Beardsley (1974) provides a suitable explanation for the appearance of internal waves associated with the advancement of a warm (less dense) front. The number of waves observed varies from one time to another and is thought to be related to the magnitude of vertical shear and altered stratification over the fortnightly tide cycle. From the aerial observations, a change of waveform was noted in areas shallower than twice the pycnocline depth. Adjacent to the Isle Verte coast the breakdown of the long wavelength internal waves resulted in the generation of a closer spaced group of waves oriented at right angles to the former ones.

Acknowledgments. This work is a contribution to the program of the Groupe Interuniversitaire de Recherches Océanographiques du Québec, which receives funding from the Department of Education, Province of Quebec and the National Research Council of Canada. An individual operating grant from the National Research Council of Canada is also acknowledged. Thanks also to Dr. E. M. Hassan who kindly provided unpublished STD data from a Bedford Institute of Oceanography cruise, and to Mr. P. Vandall for providing the aerial photograph shown herein. I also acknowledge the helpful comments of Drs. S. Prinsenberg and W. Forrester on the manuscript.

REFERENCES

Apel, J. R., H. M. Byrne, J. R. Proni and R. L. Charnell. 1975. Observations of oceanic internal waves from the Earth Resources Technology Satellite, J. Geophys. Res., *80,* 865–881.

Canadian Hydrographic Service. 1939. Tidal current charts, St. Lawrence estuary, Orleans Island to Father Point, Tidal Publ. 21, Ottawa, Canada.

Gargett, A. E. 1976. Generation of internal waves in the Strait of Georgia, British Columbia, Deep Sea Res., *23,* 17–32.

Halpern, D. 1971. Observations on short period internal waves in Massachusetts Bay. J. Mar. Res., *29,* 116–132.

Hughes, B. A. and H. L. Grant. 1978. The effect of internal waves on surface wind waves. 1. Experimental measurements. J. Geophys. Res., *83,* 443–454.

Hunkins, K. and M. Fliegel. 1973. Internal undular surges in Seneca Lake: A natural occurrence of solitons. J. Geophys. Res., *78,* 539–548.

LaFond, E. C. 1966. Internal waves, *in* Encyclopedia of Oceanography, R. W. Fairbridge, ed., New York, Reinhold.

Lee, C. Y. and R. C. Beardsley. 1974. The generation of long nonlinear internal waves in a weakly stratified shear flow. J. Geophys. Res., *79,* 453–462.

Shand, J. A. 1953. Internal waves in Georgia Strait. EOS Trans. AGU, *34,* 849–856.

Received: *27 February, 1978;* revised: *20 July, 1978.*